

## The Quark Mixing Matrix in a Composite Model

H. KATSUMATA AND Y. TOMOZAWA

*Randall Laboratory of Physics, University of Michigan,  
Ann Arbor, Michigan 48109*

Received November 29, 1982, revised February 22, 1983

The generalized mixing matrix of quarks is computed based on a composite model of quarks and leptons. Among potentials between constituent particles examined  $V(r) = Ar^A$  ( $A > 0$ ) and  $A \ln r$  ( $A > 0$ ), it is shown that potentials with exponent  $0 \leq s \leq 3$  or  $\ln r$  are consistent with current experimental data for the mixing matrix elements.

### I. INTRODUCTION

The quarks and leptons are grouped in families and generations. An important but difficult question is how many generations exist in nature and what is their mass spectrum. Apparently the mass of the quarks increases at least exponentially as a function of the generation number, while the increment for lepton masses with respect to the generation number is less drastic.

There has been a suggestion [1] that quarks and leptons are composite systems made of more fundamental objects and the generations are their excited states. If that is the case, we can eliminate some of the mysteries of generations. The number of generations may be infinite, but practically only a finite number will be observed if the mass increases exponentially with the radial quantum number. Then, some questions which should be considered are (a) what are the properties of the constituent objects and of their interactions, (b) how can the mass spectrum of the generations be understood, and (c) is it possible to compute the quark mixing matrix from the bound state wave functions? Clearly questions (b) and (c) are related to question (a).

In order to avoid the difficulty of spin  $\frac{3}{2}$  bound states without introducing large spin dependent forces, we assume that the constituents are spin 0 and spin  $\frac{1}{2}$  particles, as is suggested in [1]. Obviously, question (b), the problem of a rapidly increasing mass spectrum, is the most difficult one. This is because the mass spectrum of the excited states increases at most as  $n^2$  for a local potential model where  $n$  is the radial quantum number. (This is realized for a rigid wall potential.) Also the excited states with orbital angular momentum should have very large energy, so that one will not observe them at low energy. On the other hand, question (c) was formulated in [1], which gives a hint as to how to calculate the quark mixing matrix which is a generalization of the K-M matrix [2]. Although the final answer should

simultaneously solve all three questions stated above, one may wonder whether one can solve question (c) without confronting the difficulty of (b).

In this article, we suggest such a model and calculate the mixing matrix (Section II). Section III is devoted to a comparison with experiment and discussions.

## II. THE MODEL AND CALCULATION OF THE MIXING MATRIX

Following the suggestion of [1], we assume that the quarks of charge  $2e/3$  ( $-e/3$ ) are the  $nS_{1/2}$  excited states of the  $U(D)$  and  $B$  particles, where  $U, D$  is an isodoublet of spin  $\frac{1}{2}$  and  $B$  is an isosinglet of spin 0. (The spin assignment could be vice versa, i.e., spin of  $U, D$  and  $B$  could be 0 and  $\frac{1}{2}$ , respectively.) For the leptons,  $U(D)$  is replaced by  $N(E)$ .

The potential between the  $U, D$  and  $B$  particles is assumed to be

$$V = V_l(E) + V(r), \quad (1)$$

where  $V_l(E)$  is energy and orbital angular momentum dependent but coordinate independent and  $V(r)$  is a local potential which is responsible for making bound states. The arbitrary constant  $V_l(E)$  is added to adjust the observed mass spectrum of the generations and explain the nonappearance of the orbital angular momentum states. The local potential  $V(r)$  will be chosen to be (A) a rigid wall potential, (B) the Coulomb potential, (C) a harmonic oscillator potential for analytic computations and (D) the power potential  $V(r) = Ar^s$ ,  $A > 0$ ,  $s > 0$ , and a logarithmic potential  $V(r) = A \ln r$  for computer calculations. We will see that comparison with the experimental data seems to give some insight into the nature of the potential of the constituent particles.

Despite the energy dependence of the potential the choice of the form (1) leads to the orthogonality of wave functions  $\psi = ru_{nl}(r) Y_{lm}(\theta, \phi)$ , i.e., from the Schrödinger equation

$$-\frac{1}{2m} \left( \frac{d^2}{dr^2} - \frac{l(l+1)}{r^2} \right) u_{nl}(r) + (V_l(E_{nl}) + V(r)) u_{nl}(r) = E_{nl} u_{nl}(r), \quad (2)$$

it follows that

$$\int_0^\infty u_{nl}(r) u_{n'l'}(r) dr = \delta_{nn'}. \quad (3)$$

### A. Rigid Wall Potential

We are interested only in the  $S$ -wave excited states. The potential is

$$\begin{aligned} V &= V_0(E), & r \leq r_0, \\ &= \infty, & r \geq r_0. \end{aligned} \quad (4)$$

The normalized solution of the Schrödinger equation ( $m$  is the reduced mass)

$$\frac{d^2u}{dr^2} + 2m(E - V)v = 0, \tag{5}$$

is

$$\begin{aligned} u_n &= \frac{2}{r_0} \sin k_n r = \frac{2}{r_0} \sin \frac{n\pi r}{r_0}, & r \leq r_0, \\ u_n &= 0, & r \geq r_0, \end{aligned} \tag{6}$$

where

$$k_n = 2m(E_n - V_0(E)) = \frac{n\pi}{r_0}. \tag{7}$$

It is obvious that the solution  $\{u_n(r)\}$  is an orthonormal set. An example of  $V_0(E)$  which gives the mass spectrum of the generations is

$$2m(E - V_0(E)) = 2m\mu \ln \left( \frac{E}{E_0} \right), \tag{8}$$

where  $\mu$  and  $E_0$  are appropriate constants with the dimension of mass. Then we obtain

$$E_n = E_0 e^{n\pi/2m\mu r_0}, \tag{9}$$

which gives masses which are a geometrical series. Solving  $V_0(E)$  in Eq. (8), we have

$$V_0(E) = E - \mu \left( \ln \left( \frac{E}{E_0} \right) \right)^2. \tag{10}$$

If the mass spectrum is not a geometrical series, it is easy to adjust  $V_0(E)$  to accommodate the real situation.

The parameters  $M$ ,  $r_0$ ,  $\mu$ , and  $E_0$  could be slightly different for the  $(UB)_n = u_n$  and  $(DB)_n = d_n$  bound states, because of violation of isospin invariance (the parameters for the latter are denoted by the primed quantities). This then leads to nonorthogonality between the  $\{u_n\}$  and  $\{d_n\}$  wave functions and their overlap integrals give the mixing matrix [1].

Assuming that  $r_0 < r'_0$ , the matrix element of the mixing matrix  $U = \{a_{nl}\}$  can be calculated as

$$\begin{aligned} a_{nl} &= \int_0^{r_0} \frac{2}{r_0} \frac{2}{r'_0} \sin \left( \frac{n\pi r}{r_0} \right) \sin \left( \frac{l\pi r}{r'_0} \right) dr \\ &= \frac{1}{\pi} \frac{1}{r_0 r'_0} \frac{\sin(n\pi - l\pi r_0/r'_0)}{((n/r_0) - (l/r'_0))} - \frac{\sin(n\pi + l\pi r_0/r'_0)}{((n/r_0) + (l/r'_0))} \\ &= (-1)^{n+1} \frac{2n}{\pi} \sqrt{z} \frac{\sin(l\pi z)}{n^2 - l^2 z^2}, \end{aligned} \tag{11}$$

where

$$z = r_0/r'_0. \tag{12}$$

The matrix  $U$  is an orthogonal matrix which follows from the orthonormality of the set  $\{u_n\}$  and  $\{d_n\}$ , i.e.,

$$\sum_{l=1}^{\infty} \frac{2n\sqrt{z}}{\pi} \frac{\sin l\pi z}{n^2 - l^2 z^2} \frac{2n'\sqrt{z}}{\pi} \frac{\sin l'\pi z}{n'^2 - l'^2 z^2} = \delta_{nn'},$$

(13)

and

$$\sum_{n=1}^{\infty} \frac{2n\sqrt{z}}{\pi} \frac{\sin l\pi z}{n^2 - l^2 z^2} \frac{2n\sqrt{z}}{\pi} \frac{\sin l'\pi z}{n^2 - l'^2 z^2} = \delta_{ll'}.$$

We have neglected small CP violating phases. The physical meaning of the matrix elements  $\{a_{nl}\}$  is exhibited by showing the weak doublets

|   |   |
|---|---|
| $u$   | $c$   |
| $a_{11}d + a_{12}s + a_{13}b + a_{14}b' + \dots,$ | $a_{21}d + a_{22}s + a_{23}b + a_{24}b' + \dots,$ |
| $t$   | $t'$  |
| $a_{31}d + a_{32}s + a_{33}b + a_{34}b' + \dots,$ | $a_{41}d + a_{42}s + a_{43}b + a_{44}b' + \dots.$ |

(14)

We shall fix the parameter  $z$  using the experimental value of the Cabibbo angle

$$a_{12} = \frac{2\sqrt{z}}{\pi} \frac{\sin 2\pi z}{1 - 4z^2} = \sin \theta_C = 0.219, \tag{15}$$

which gives

$$z \equiv r_0/r'_0 = 0.867. \tag{16}$$

Then all the matrix elements of  $U$  are determined and given by

$$U = \begin{pmatrix} 0.969 & 0.219 & -0.0977 & 0.0555 \dots \\ -0.148 & 0.885 & 0.407 & -0.147 \dots \\ 0.0875 & -0.220 & 0.756 & 0.585 \dots \\ -0.0631 & 0.135 & -0.244 & 0.594 \dots \end{pmatrix}, \tag{17}$$

These results should be compared to a phenomenological determination of the mixing matrix

$$|a_{11}| = 0.9737 \pm 0.0025, \quad |a_{12}| = 0.219 \pm (0.002; 0.011),$$

$$|a_{13}| = 0.06 \pm 0.06, \tag{18a}[3]$$

$$0.192 < |a_{21}| < 0.34, \quad |a_{22}| = 0.8 \pm 0.2, \quad |a_{23}| > 0.01, \tag{18b}[4]$$

and more recently

$$\frac{|a_{12}|}{|a_{13}|} < 0.2. \tag{18c)}{5}$$

It is clear that we have to use a phenomenological analysis without using the K–M angles parametrization, since our matrix  $U$  is infinite dimensional.

We may add that we have a few more alternative solutions for the  $U$  matrix. The value  $z = 0.15$  satisfies Eq. (15), but it gives  $a_{11} = 0.123$ . Also  $U^T$  gives possible solutions. Writing  $a'_{nl} = (-1)^{n+l} a_{ln}$ , the condition  $a'_{12}(z) = 0.219$  leads to  $z = 0.765$  or  $0.443$ , which in turn gives  $a'_{11} = 0.903$  or  $0.519$ . These three solutions do not give acceptable values of  $a_{11}$  or  $a'_{11}$  and therefore are discarded.

**B. The Coulomb Potential**

For an alternative potential, we use the Coulomb potential. The  $nS$  wave functions are

$$\begin{aligned} R_{10} &= 2\alpha^{3/2} \exp(-ar), \\ R_{20} &= -2(\frac{1}{2}\alpha)^{3/2} (1 - \frac{1}{2}ar) \exp(-\frac{1}{2}ar), \\ R_{30} &= 2(\frac{1}{3}\alpha)^{3/2} (1 - \frac{2}{3}ar + \frac{2}{27}\alpha^2 r^2) \exp(-\frac{1}{3}ar), \\ R_{40} &= -\frac{1}{4}(\alpha)^{3/2} (1 - \frac{3}{4}ar + \frac{1}{8}\alpha^2 r^2 - \frac{1}{192}\alpha^3 r^3) \exp(-\frac{1}{4}ar), \end{aligned} \tag{19}$$

where  $R_{n0} = u_n/r$ . For the set  $\{d_n/r\}$ ,  $\alpha$  should be replaced by  $\alpha'$ . The matrix elements of  $U$  are easily calculated,

$$a_{nl} = \int_0^\infty u_n(r) d_l(r) dr. \tag{20}$$

Using

$$z = \alpha/\alpha', \tag{21}$$

we obtain

$$\begin{aligned} a_{11} &= \frac{8z^{3/2}}{(1+z)^3}, & a_{12} &= 8 \left(\frac{z}{2}\right)^{3/2} \frac{(1-z)}{(1/2+z)^4}, \\ a_{13} &= -\frac{8}{3} \left(\frac{z}{3}\right)^{3/2} \frac{(1-z)(3z-1)}{(1/3+z)^5}, \\ a_{14} &= -\frac{1}{2} \frac{z^{3/2}}{(z+1/4)^6} [2(z+1/4)^3 - 9/2(z+1/4)^2 + 3(z+1/4) - 5/8], \\ a_{22} &= \frac{16z^{3/2}}{(1+z)^5} (6z - (1+z)^2), \end{aligned}$$

$$\begin{aligned}
 a_{23} &= \frac{2}{9} \frac{1}{(1/3 + z/2)^6} (z/6)^{3/2} (1-z)(-4 + 36z - 2z^2), \\
 a_{24} &= \frac{8}{(z + 1/2)^7} \left(\frac{z}{2}\right)^{3/2} [(z + 1/2)^4 - 3(z + 3/2)(z + 1/2)^3 + 6(1 + 3z)(z + 1/2)^2 \\
 &\quad - \frac{5}{2} (1 + 12z)(z + 1/2) + 15z], \\
 a_{33} &= \frac{8z^{3/2}}{(1+z)^7} [160z^2 - 5(1+z)^4 + 8(1+z^2 - 4z)(1+z)^2], \\
 a_{34} &= -\frac{1}{(z/3 + 1/4)^8} \left(\frac{z}{2}\right)^{3/2} \left[ \left(\frac{z}{3} + \frac{1}{4}\right)^5 - (2z + 9/4) \left(\frac{z}{3} + \frac{1}{4}\right)^4 \right. \\
 &\quad + \left(\frac{8}{9}z^2 + 6z + \frac{3}{2}\right) \left(\frac{z}{3} + \frac{1}{4}\right)^3 \\
 &\quad \left. - \left(\frac{10}{3}z^2 + 5z + \frac{5}{16}\right) \left(\frac{z}{3} + \frac{1}{4}\right)^2 + \left(\frac{5}{4}z + \frac{10}{3}z^2\right) \left(\frac{z}{3} + \frac{1}{4}\right) - \frac{35}{36} \right], \quad (22)
 \end{aligned}$$

and

$$\begin{aligned}
 a_{44} &= \frac{32z^{3/2}}{(1+z)^9} [-2(1+z)^6 + 3(2 + 2z^2 + 9z)(1+z)^4 \\
 &\quad - 5(1+z^3 + 18z(1+z))(1+z)^3 + 90(z(1+z^2) + 4z^2)(1+z)^2 \\
 &\quad - 420z^2(1+z)^2 + 560z^3].
 \end{aligned}$$

To determine the rest of the  $a_{ni}$ 's we make use of the following relationship:

$$a_{ni}(z) = a_{in}(z^{-1}). \quad (23)$$

The parameter  $z$  is determined by the Cabibbo angle, as before, giving

$$z = 0.720. \quad (24)$$

We obtain the numerical values of the  $U$  matrix

$$\begin{aligned}
 U = & \begin{array}{cccc}
 0.961 & 0.218 & -0.0785 & 0.0454 \dots, \\
 -0.141 & 0.884 & 0.402 & -0.112 \dots, \\
 0.0683 & -0.234 & 0.764 & 0.570 \dots, \\
 -0.0426 & 0.126 & -0.281 & 0.608 \dots.
 \end{array} \quad (25)
 \end{aligned}$$

An alternative solution is obtained by an unlikely value  $z = 0.0035$ , but was discarded since it leads to an unacceptable value for  $a_{11}$  ( $= 0.451$ ). Comparing matrices (17) and (25), we notice a striking similarity despite the large difference

between the potentials used. One might think that qualitative features of the  $U$  matrix may be insensitive to the detailed form of the potential  $V(r)$ . We will show that this is not the case. The next example, a harmonic oscillator potential, gives a markedly different prediction for the mixing matrix.

### C. Harmonic Oscillator Potential

For a harmonic oscillator potential

$$V(r) = \frac{m\omega^2}{2} r^2, \quad (26)$$

we list the radial wave functions  $R_n(r)$  for the first four  $S$ -states.

$$\begin{aligned} R_{10}(r) &= (4k^3/\sqrt{\pi}) e^{-\rho^2/2}, \\ R_{20}(r) &= -(8k^3/3\sqrt{\pi}) e^{-\rho^2/2} (3/2 - \rho^2), \\ R_{30}(r) &= (2^4 2! k^3 / 5!! \sqrt{\pi}) e^{-\rho^2/2} \left( \frac{15}{8} - \frac{5}{2} \rho^2 + \frac{\rho^4}{2} \right), \\ R_{40}(r) &= -(2^5 3! k^3 / 7!! \sqrt{\pi}) e^{-\rho^2/2} \left( \frac{35}{16} - \frac{35\rho^2}{8} + \frac{7\rho^4}{4} - \frac{\rho^6}{6} \right), \end{aligned} \quad (27)$$

where

$$k = \sqrt{m\omega},$$

and

$$(28)$$

$$\rho = kr.$$

Denoting the parameter for the down quark by  $k'$ , we can compute the mixing matrix by the overlap integrals as before. The results are

$$\begin{aligned} a_{11} &= (\sin \theta)^{3/2}, \\ a_{12} &= \sqrt{3/2} (\sin \theta)^{3/2} \cos \theta, \\ a_{13} &= \sqrt{30/16} (\sin \theta)^{3/2} \cos^2 \theta, \\ a_{14} &= \sqrt{35/16} (\sin \theta)^{3/2} \cos^3 \theta, \\ a_{22} &= (\sin \theta)^{3/2} (1 - \frac{5}{2} \cos^2 \theta), \\ a_{23} &= \sqrt{5} (\sin \theta)^{3/2} \cos \theta (1 - \frac{7}{4} \cos^2 \theta), \\ a_{24} &= \sqrt{210/4} (\sin \theta)^{3/2} \cos^2 \theta (1 - \frac{3}{2} \cos^2 \theta), \\ a_{33} &= (\sin \theta)^{3/2} (1 - 7 \cos^2 \theta + \frac{63}{8} \cos^4 \theta), \\ a_{34} &= \frac{21}{2} (\sin \theta)^{3/2} \cos \theta (1 - \frac{9}{2} \cos^2 \theta + \frac{33}{8} \cos^4 \theta), \\ a_{44} &= (\sin \theta)^{3/2} (1 - \frac{27}{2} \cos^2 \theta + \frac{297}{8} \cos^4 \theta - \frac{429}{16} \cos^6 \theta), \end{aligned} \quad (29)$$

where the parameterization

$$z = \frac{k}{k'} = \tan \frac{\theta}{2}, \quad \frac{2z}{1+z^2} = \sin \theta, \quad \frac{1-z^2}{1+z^2} = \cos \theta, \quad (30)$$

has been used. The matrix element  $a_{nl}$  is obtained by interchanging the parameter  $k \leftrightarrow k'$ , or equivalently  $\theta \rightarrow \pi - \theta$  in  $a_{ln}$ . From Eq. (29), it follows then that the  $U$  matrix satisfies the symmetry property

$$a_{nl}(\theta) = a_{ln}(\pi - \theta) = (-1)^{n+l} a_{ln}(\theta), \quad (31)$$

i.e., the off-diagonal elements  $a_{nl}$  are symmetric (skew symmetric) if  $n+l$  is even (odd). This is markedly different from the results for potentials considered in the previous subsections.

The determination of the parameter  $\theta$  by the Cabibbo angle ( $a_{12}$ ) leads to

$$\sin \theta = 0.983,$$

or

$$z = \tan \frac{\theta}{2} = 0.831,$$

(32)

TABLE I

The Mixing Matrix<sup>a</sup>  $U = (a_{ij})$  for Power Potentials  $V(r) = Ar^s$  ( $As < 0$ ) and Logarithmic Potential  $V(r) =$

| $S$           | $a_{11}$ | $a_{13}$ | $a_{14}$ | $a_{21}$ | $a_{22}$ | $a_{23}$ | $a_{24}$ |
|---------------|----------|----------|----------|----------|----------|----------|----------|
| -1            | 0.961    | -0.0785  | 0.0454   | -0.141   | 0.884    | 0.402    | -0.1     |
| 0             | 0.9742   | -0.0425  | 0.0241   | -0.183   | 0.900    | 0.392    | -0.0     |
| (Logarithmic) |          |          |          |          |          |          |          |
| .1            | 0.9746   | -0.0376  | 0.0213   | -0.186   | 0.900    | 0.392    | -0.0     |
| .6            | 0.9756   | -0.0129  | 0.00961  | -0.197   | 0.900    | 0.388    | 0.0      |
| .8            | 0.9757   | -0.00349 | 0.00715  | -0.201   | 0.899    | 0.387    | 0.0      |
| .9            | 0.9757   | 0.00111  | 0.00613  | -0.202   | 0.899    | 0.386    | 0.0      |
| 1             | 0.9757   | 0.00560  | 0.00564  | -0.204   | 0.898    | 0.385    | 0.0      |
| 2             | 0.9746   | 0.0450   | 0.00892  | -0.219   | 0.892    | 0.376    | 0.1      |
| 3             | 0.9726   | 0.0744   | 0.0227   | -0.232   | 0.885    | 0.367    | 0.1      |
| 4             | 0.9700   | 0.0959   | 0.0395   | -0.243   | 0.876    | 0.359    | 0.1      |
| 5             | 0.967    | 0.111    | 0.0556   | -0.253   | 0.867    | 0.352    | 0.2      |
| 10            | 0.953    | 0.141    | 0.102    | -0.296   | 0.822    | 0.324    | 0.2      |
| 20            | 0.932    | 0.143    | 0.113    | -0.349   | 0.757    | 0.290    | 0.2      |
| 30            | 0.921    | 0.140    | 0.108    | -0.375   | 0.723    | 0.274    | 0.1      |
| 50            | 0.912    | 0.136    | 0.103    | -0.395   | 0.696    | 0.261    | 0.1      |
| 100           | 0.910    | 0.135    | 0.100    | -0.404   | 0.689    | 0.258    | 0.1      |
| Rigid Wall    | 0.969    | -0.0977  | 0.0555   | -0.148   | 0.885    | 0.407    | -0.1     |

<sup>a</sup>  $a_{12} = \sin \theta_c = 0.219$  is an input.



and the  $U$  matrix

$$U = \begin{pmatrix} 0.9746 & \underline{0.219} & 0.0450 & 0.00892 \dots, \\ -0.219 & 0.892 & 0.376 & 0.113 \dots, \\ 0.0450 & -0.376 & 0.753 & 0.495 \dots, \\ -0.00892 & 0.113 & -0.495 & 0.571 \dots. \end{pmatrix} \quad (33)$$

D. Power Potentials with an Arbitrary Exponent

For a power potential

$$V(r) = Ar^s \quad (As > 0), \quad (34)$$

and a logarithmic potential

$$V(r) = A \ln r \quad (A > 0), \quad (35)$$

computer calculations are performed to obtain the mixing matrix elements. The results are given in Table I.

TABLE I—Continued.

| $a_{31}$ | $a_{32}$ | $a_{33}$ | $a_{34}$ | $a_{41}$  | $a_{42}$ | $a_{43}$ | $a_{44}$ | $a_{13}/a_{23}$ |
|----------|----------|----------|----------|-----------|----------|----------|----------|-----------------|
| 0683     | -0.234   | 0.764    | 0.570    | -0.0426   | 0.126    | -0.281   | 0.608    | -0.195          |
| 0890     | -0.301   | 0.776    | 0.547    | -0.0541   | 0.156    | -0.376   | 0.610    | -0.108          |
| 0885     | -0.306   | 0.775    | 0.545    | -0.0515   | 0.155    | -0.384   | 0.609    | -0.0959         |
| 0790     | -0.329   | 0.771    | 0.533    | -0.0421   | 0.150    | -0.419   | 0.601    | -0.0333         |
| 0747     | -0.337   | 0.769    | 0.528    | -0.0367   | 0.146    | -0.432   | 0.597    | -0.00902        |
| 0726     | -0.340   | 0.768    | 0.525    | -0.0337   | 0.144    | -0.438   | 0.595    | 0.00288         |
| 0701     | -0.344   | 0.767    | 0.522    | -0.0314   | 0.142    | -0.444   | 0.593    | 0.0145          |
| 0450     | -0.376   | 0.753    | 0.595    | -0.00892  | 0.113    | -0.495   | 0.571    | 0.119           |
| 0210     | -0.402   | 0.738    | 0.468    | 0.00451   | 0.0831   | -0.534   | 0.546    | 0.203           |
| 00512    | -0.424   | 0.720    | 0.445    | 0.0105    | 0.0569   | -0.568   | 0.518    | 0.267           |
| 0165     | -0.445   | 0.701    | 0.424    | 0.0120    | 0.0351   | -0.596   | 0.489    | 0.316           |
| 0657     | -0.523   | 0.613    | 0.342    | -0.000557 | -0.0281  | -0.699   | 0.361    | 0.436           |
| 0949     | -0.611   | 0.499    | 0.255    | -0.0156   | -0.0594  | -0.794   | 0.213    | 0.494           |
| 02       | -0.650   | 0.443    | 0.217    | -0.0177   | -0.0597  | -0.830   | 0.150    | 0.511           |
| 05       | -0.679   | 0.401    | 0.191    | -0.0166   | -0.0532  | -0.851   | 0.106    | 0.522           |
| 06       | -0.696   | 0.390    | 0.183    | -0.0156   | 0.0497   | -0.870   | 0.0938   | 0.524           |
| 0875     | -0.220   | 0.756    | 0.585    | -0.0631   | 0.135    | -0.244   | 0.594    | -0.240          |

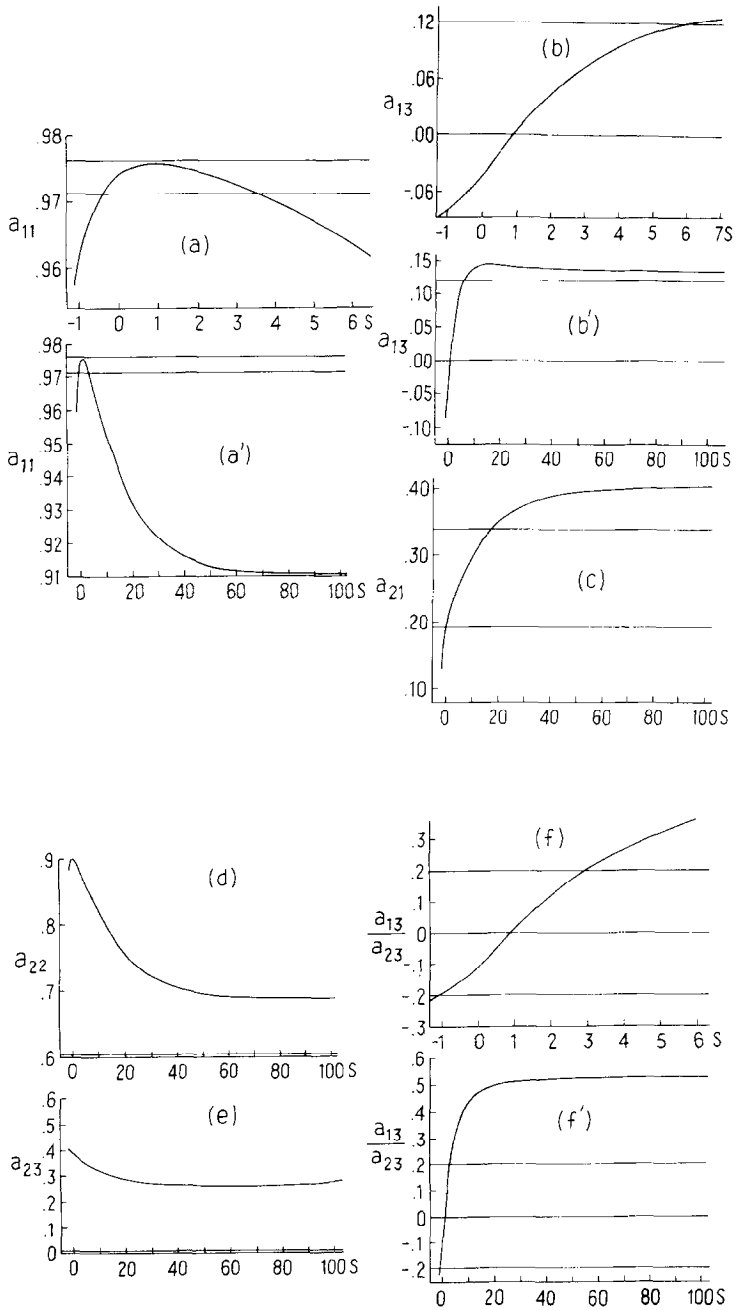


FIG. 1. Sketch of the  $s$  dependence of the matrix element  $a_{ij}$ , where  $s$  is the exponent of the potential  $V(r) = Ar^s$ . The two horizontal lines represent experiment bounds. (a)  $|a_{11}|$ , (b)  $|a_{13}|$ , (c)  $|a_{21}|$ , (d)  $|a_{22}|$ , (e)  $|a_{23}|$ , and (f)  $|a_{13}|/|a_{23}|$ .

III. COMPARISON WITH EXPERIMENT AND DISCUSSION

In order to compare the results of the previous section with experimental values of the mixing matrix (18), we show a sketch of  $a_{nl}$  ( $n \leq 2, l \leq 3$ ) and the ratio

$$\left| \frac{a_{13}}{a_{23}} \right| = \frac{\text{amplitude}(b \rightarrow u)}{\text{amplitude}(b \rightarrow c)}, \tag{36}$$

as a function of the power of potential  $V(r) = Ar^s$  (Fig. 1). It is quite clear that the prediction of the power potential is consistent, with an exponent  $0 \lesssim s \lesssim 3$ , with the accurate value of  $|a_{11}|$  and the upperbound of the ratio  $|a_{13}|/|a_{23}|$ . In other words, the harmonic oscillator potential, a linear potential, and a logarithmic potential are acceptable while a Coulomb potential and a rigid wall potential are in conflict with experimental data, as is seen in Fig. 1. Notice that the potentials which are mentioned above as successful are also phenomenologically acceptable potentials for quarkonium [6–9]. A further comparison of experimental data and our prediction might shed some light on the nature of the potential among constituent particles in the composite model.

Needless to say, the important questions of explaining the generation spectra and absence of orbital angular momentum states are left open for further investigations.

A similar work was done independently by Terazawa and Akama [10, 11], who calculated the mixing matrix for the relative Dirac particle with the Coulomb potential and the rigid wall potential. The results obtained are remarkably close to our results for these potentials. In other words, the relativistic corrections of this kind for the mixing matrix are relatively small. They did not study the potential dependence of the mixing matrix, as is done in this article, since the relativistic equation (the Dirac or the Klein–Gordon equation) with the minimum interaction given by power potentials does not have bound state solutions.

APPENDIX: GENERATION MASS SPECTRA

The mass ratios between the generations are given by

$$\frac{m_\mu}{m_e} = 207, \quad \frac{m_\tau}{m_\mu} = 17, \tag{A.1}$$

$$\frac{m_s}{m_d} = \frac{150}{5 \sim 10} = 30 \sim 15, \quad \frac{m_b}{m_s} \approx \frac{4.5}{0.15} \approx 30. \tag{A.2}$$

As is seen above, the quark masses increase as a geometrical series or even stronger, while the lepton masses are not quite a geometrical series. As was pointed out earlier, it is easy to adjust  $V_0(E)$  to this situation. However, the disparity between leptons and quarks is striking and should be seriously considered.

Assuming that the quark masses increase geometrically, we may predict the mass of the top quark  $t, t'$ ,

$$m_t = \frac{m_c^2}{m_u} = \frac{(1.5)^2}{\sim 0.01} \approx 225 \text{ GeV},$$

$$m_{t'} = \frac{m_c^3}{m_u^2} = 3.4 \times 10^5 \text{ GeV},$$
(A.3)

and

$$m_{b'} = \frac{m_b^2}{m_s} = 135 \text{ GeV, etc.}$$

Again the disparity among the masses of the  $\{u_n\}$  and  $\{d_n\}$  series looks peculiar. The number of top and bottom quarks below  $10^{14}$  GeV may be estimated by

$$m_c \left( \frac{m_c}{m_u} \right)^{n_t} = 10^{14},$$
(A.4)

and

$$m_b \left( \frac{m_b}{m_s} \right)^{n_b-1} = 10^{14},$$

giving

$$n_t \cong 6,$$

and

$$(A.5)$$

$$n_b \cong 10$$

$[n_t(n_b)$  is the number of  $t, t', \dots (b, b', \dots)]$ . In any event, the mass spectrum of the generation is an entirely open question.

There has been discussed a stringent constraint on the mass spectrum of leptons and quarks due to the value of the  $\rho$  parameter ( $\rho = m_W/m_Z \cos \theta_w$ , where  $m_w, m_z$ , and  $\theta_w$  are the masses of the  $W$ -boson, the  $Z^0$ -boson, and the weak interaction angle respectively) [12]. This will be useful information for constructing a more sophisticated composite model.

#### ACKNOWLEDGMENTS

The original version of this work was done when Vladimir Visnjic visited Michigan in Fall 1980 and was distributed as internal report UM HE 81-3. The authors are greatly indebted to him for stimulating

discussions and collaborations. The authors wish to thank Martinus Veltman for encouragement, Bob Levine and David Unger for critical comments and reading the manuscript, and Bob Shrock for useful information. The work is supported in part of the U.S. Department of Energy.

## REFERENCES

1. V. VISNJIC-TRJANTAFILLOU, *Phys. Rev. D* **25** (1982), 248; M. VELTMAN, in "Proceedings of the 1979 International Symposium on Lepton and Photon Interactions at High Energies" (T. B. W. Kirk and H. D. I. Abarbanel, Eds.), p. 529, Fermilab, 1979; for earlier references, see, e.g., O. W. GREENBERG, *Amer. J. Phys.* **50** (1982), 1074.
2. M. KOBAYASHI AND T. MASKAWA, *Prog. Theor. Phys.* **49** (1973), 652.
3. R. E. SHROCK, S. B. TREIMAN, AND L. L. WANG, *Phys. Rev. Lett.* **42** (1979), 1589.
4. S. PAKVASA, S. F. TUAN, AND J. J. SAKURAI, UH-511-427-80, 1980.
5. See, e.g., L. L. CHAU, in "Proceedings of the Eight International Workshop on Weak Interactions and Neutrinos" (A. Morales, Ed.), Javea, Spain, 1982, to be published.
6. E. EICHEN *et al.*, *Phys. Rev. D* **17** (1978), 3090; **21**(1980), 203.
7. M. MACHACEK AND Y. TOMOZAWA, *Prog. Theor. Phys.* **58** (1977) 1980; *Ann. Phys. (NY)* **110** (1978), 407; C. QUIGG AND J. L. ROSNER, *Phys. Lett. B* **71** (1977), 153; A. MARTIN, *Phys. Lett. B* **93** (1980), 338.
8. R. D. CARLITZ AND D. R. CREAMER, *Ann. Phys. (NY)* **118** (1979), 429; J. L. RICHARDSON, *Phys. Lett. B* **82** (1979), 272; R. LEVINE AND Y. TOMOZAWA, *Phys. Rev. D* **19** (1979), 1572.
9. R. LEVINE AND Y. TOMOZAWA, *Phys. Rev. D* **21** (1980), 840; W. BUCHMULLER AND S. H. H. TYE, *Phys. Rev. D* **24** (1981), 132.
10. Y. TOMOZAWA, UM He 81-3 1981, unpublished; H. TEREZAWA AND K. AKAMA, *Phys. Lett. B* **101** (1981), 190.
11. Y. TOMOZAWA, *Phys. Lett. B* **104** (1981), 136; in "Proceedings of the INS Physics Symposium on Quarks and Leptons" (K. Fujikawa *et al.*, Eds.), p.319, 1981; H. TERAZAWA, in "Proceedings INS Symposium on Quark and Lepton Physics" (Fujikawa *et al.*, Eds.), p. 296, 1981.
12. M. VELTMAN, *Nuclear Phys. B* **123** (1977), 89.